3D Macro Element for Soil Structure Interaction

Stéphane Grange, Panagiotis Kotronis, J. Mazars

4ICEGE Thessaloniki-GREECE 2007

4th International Conference on
Earthquake Geotechnical Engineering
June 25-28, 2007
Paper No. 1308

A 3D MACRO ELEMENT FOR SOIL STRUCTURE INTERACTION

Stéphane GRANGE[1], Panagiotis KOTRONIS[2], and Jacky MAZARS[3]

ABSTRACT

This paper presents a 3D non linear interface element able to compute Soil Structure Interaction (SSI). Several approaches exist to take this phenomenon into account: the following work is based on the "macro element" concept and is inspired on the work of (Crémer, 2001). The particularity of the macro element lies in the fact that the movement of the foundation is entirely described by a system of generalised variables (forces and displacements) defined in the foundation centre. The non linear behaviour of the soil is reproduced using the classical theory of plasticity. The failure surface is defined using an adequate overturning mechanism according to the work of (Pecker, 1997).
The element is able to simulate the 3D behaviour of a circular rigid shallow foundation under cyclic and dynamic loading considering rocking. It is implemented into FedeasLab, a finite element Matlab toolbox. Comparisons with experimental results under monotonic static (Gottardi et al., 1999), cyclic (TRISEE, 1998), and dynamic conditions (Combescure et al., 2000, CAFEEL-ECOEST/ICONS, 2001) show the good performance of the approach.

Keywords: soil structure interaction, macro-element, foundation, plasticity, uplift, rocking.

INTRODUCTION

In structural engineering, Soil Structure Interaction (SSI) is an important phenomenon that has to be taken into account. Experimental results on the CAMUS IV structure (Combescure et al., 2000, CAFEEL-ECOEST/ICONS, 2001) showed that non linearities at the soil level (plasticity) and between the soil and the foundation (rocking and uplift of the foundation) result often to an isolation of the structure and thus to a reduction of the forces and the moments developed at its base during an earthquake. Maximum values of stresses are limited because of larger energy dissipation but more important displacements are generated at the top.

In order to study the SSI, several methods exist: the macro element approach consists in condensing all non linearities into a finite domain and works with generalised variables (forces and displacements) that allow simulating in a simplified way the behavior of shallow foundations. Several 2D macro elements exist in the literature: (Nova et al., 1991), (Cassidy et al., 2002), (Crémer, 2001), (Crémer et al., 2001), (Crémer et al., 2002), (Di Prisco et al., 2006). The 2D macro element developed by Crémer can be used for static/cyclic but also dynamic loading (i.e. earthquake) applied in the horizontal direction, considering the plasticity of the soil and the rocking and uplift of the foundation.

Inspired on her work, a new 3D macro element is developed hereafter. The goal is to compute the 3D behavior of a circular shallow and rigid foundation lying on an infinite space submitted to a static or a

[1] PhD student, Laboratoire 3S-R Sols Solides Structures – Risques & research network VOR, Grenoble Universités, France, Email: Stephane.Grange@hmg.inpg.fr
[2] Assistant professor, Laboratoire 3S-R Sols Solides Structures – Risques & research network VOR, Grenoble Universités, France,, Email: Panagiotis.Kotronis@inpg.fr
[3] Professor, Laboratoire 3S-R Sols Solides Structures – Risques & research network VOR, Grenoble Universités, France, Email: Jacky.Mazars@inpg.fr

dynamic loading. In the current version the macro element takes into account the plasticity of the soil and the rocking of the structure. It is implemented into FedeasLab, a finite element Matlab toolbox developed by Pr. F. Filippou and his co-workers in UC Berkeley (Filippou et al., 2004).

After the mathematical description of the macro element, numerical results compared with experimental tests under monotonic static (Gottardi et al., 1999), cyclic (TRISEE, 1998) and dynamic (Combescure et al., 2000, CAFEEL-ECOEST/ICONS, 2001) loadings are provided to show the good performance of the approach.

SHAPE OF THE FOUNDATION AND ASSOCIATED KINEMATIC VARIABLES

In order to simplify the problem, the foundation studied hereafter is considered circular (Figure 1). Because of the symmetry of revolution, the horizontal loads in the directions *x* and *y* are computed in a similar way. Furthermore, it is easier to reproduce the interaction between horizontal forces and moments. Being a macro element, the foundation is supposed infinitely rigid and all non linearties are condensed in a representative point: its centre. Within that framework it is appropriate to work with generalized (global) variables: the vertical force V, horizontal forces H_x, H_y, and moments M_x, M_y but also the corresponding displacements: vertical settlement u_z, horizontal displacements u_x, u_y, and rotations θ_x, θ_y. Torque moment (M_z) is not taken into account by the model.

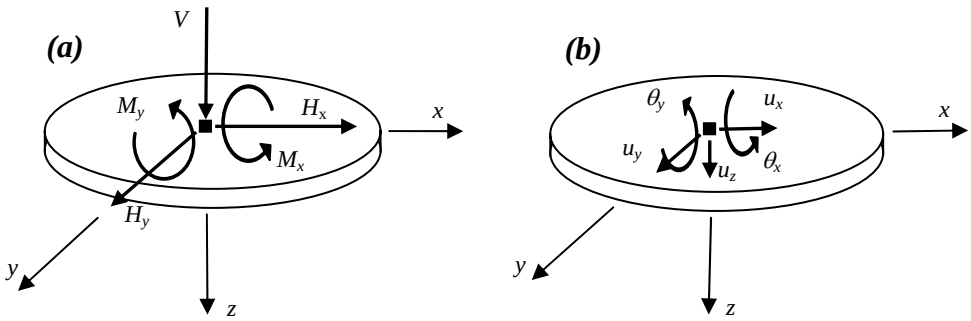

Figure 1. Shape of the foundation and generalized variables: *(a)* forces and *(b)* displacements

TWO NON LINEAR MECHANISMS: PLASTICITY AND UPLIFT

Decomposition of the non linear mechanisms

For the general case three different mechanisms must be taken into account when using a 3D SSI macro element: elasticity, plasticity of the soil and uplift of the foundation. The total displacement must thus be decomposed as a sum of the elastic, plastic and uplift part. Plasticity and uplift are coupled, as it is clearly shown hereafter.

Definition of the uplift of the foundation

Uplift is the result of rocking, i.e. the fact that the foundation rotates according to θ_x or θ_y (a part of the foundation looses contact with the soil), and a negative vertical displacement of the centre of the foundation (Figure 2). In order to compute uplift, the simple plasticity of the soil is not sufficient and a new non linear mechanism must be introduced to the macro element.

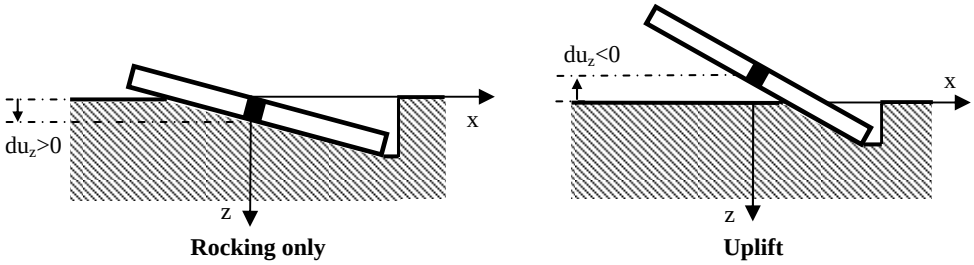

Figure 2. Rocking and uplift

In its current version the 3D macro element is able to take into account the elasticity, the plasticity of the soil and the rocking of the foundation. The negative vertical displacement of the centre of the foundation can not be calculated. The part of the foundation having no contact with the soil is assumed without stresses.

The plasticity mechanism developed in the soil is strongly influenced by the rocking (and the uplift) of the foundation. As it is shown in Figure 3, rocking leads to a non-symmetrical plasticity: when the foundation undergoes a loading in the right direction ($\dot{M} < 0$ - with (.) the sign of the derivative with respect to time), it is considered that only the soil under the right part of the foundation is plastified, no stresses are developed under the left part. When the sign of the loading is reversed ($\dot{M} > 0$), only the soil under the left part of the foundation is plastified. Under the right part, the soil remains in the same plastic state reached during the previous phase. If a third loading is applied at the right direction ($\dot{M} < 0$), the soil under the right part of the foundation is again plastified, starting from the plastic state (and with the same slope) obtained during the first phase.

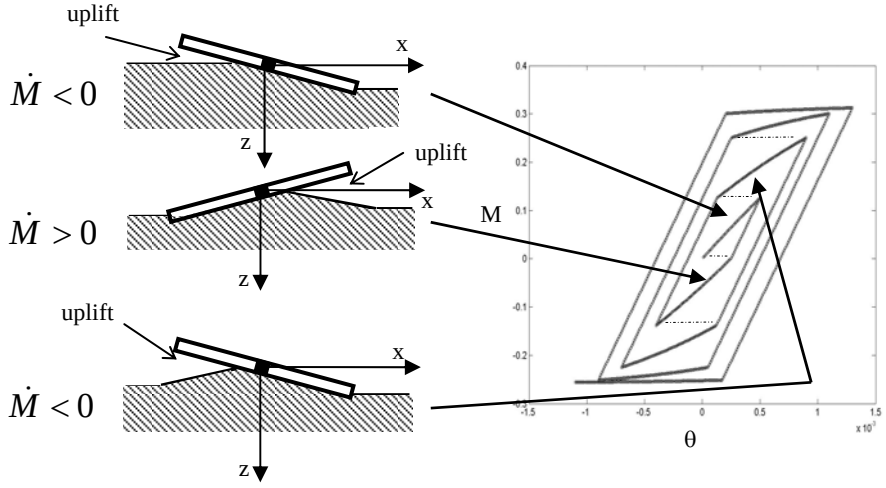

Figure 3. Influence of the rocking (and the uplift) on the plasticity mechanism

MATHEMATICAL DESCRIPTION OF THE 3D MACRO ELEMENT

Elastic behavior

The constitutive law can be written as: $\vec{F} = K^{el}\left(\vec{u} - \vec{u}^{\,pl}\right)$ where the displacement and force vectors are dimensionless:

$$\vec{F} = \begin{pmatrix} V' \\ H'_x \\ M'_y \\ H'_y \\ M'_x \end{pmatrix} = \frac{1}{\frac{\pi D^2}{4} q_{\max}} \begin{pmatrix} V \\ H_x \\ \frac{M_y}{D} \\ H_y \\ \frac{M_x}{D} \end{pmatrix}, \text{ and } \vec{u} = \begin{pmatrix} u'_z \\ u'_x \\ \theta'_y \\ u'_y \\ \theta'_x \end{pmatrix} = \frac{1}{D} \begin{pmatrix} u_z \\ u_x \\ D\theta_y \\ u_y \\ D\theta_x \end{pmatrix} \quad (1)$$

Where D is the diameter and $q_{\max}$ the ultimate bearing capacity of the foundation.

Thanks to the circular shape of the foundation, the stiffnesses corresponding to both horizontal displacements are the same. The same stands for the rotations. Using the dimensionless notation presented previously, the following dimensionless stiffness matrix is found (S being the surface of the foundation):

$$K^{el} = \begin{pmatrix} K'^{el}_{zz} & 0 & 0 & 0 & 0 \\ 0 & K'^{el}_{hh} & 0 & 0 & 0 \\ 0 & 0 & K'^{el}_{\theta\theta} & 0 & 0 \\ 0 & 0 & 0 & K'^{el}_{hh} & 0 \\ 0 & 0 & 0 & 0 & K'^{el}_{\theta\theta} \end{pmatrix} \quad (2)$$

With $K'^{el}_{zz} = \frac{K^{el}_{zz} D}{S q_{\max}}$, $K'^{el}_{hh} = \frac{K^{el}_{hh} D}{S q_{\max}}$, and $K'^{el}_{\theta\theta} = \frac{K^{el}_{\theta\theta}}{D S q_{\max}}$

The elastic stiffness matrix is calculated using the real part of the static impedances of the foundation (Gazetas, 1991).

Plastic behavior

Failure criterion

The failure criterion is defined for an overturning mechanism with uplift. It comes from the works of (Pecker, 1997) and it has been used already in the 2D macro element of (Crémer, 2001). This criterion was initially developed for a shallow strip and rigid foundation in 2D lying on a half space of homogeneous cohesion. However, (Gottardi et al., 1999) showed that the shapes of the load and failure surfaces for a circular footing are very similar.

Thanks to the symmetry of revolution, the adaptation in 3D is very simple and consists in adding 2 terms in relation with the horizontal force H'_x and the moment M'_y to obtain a 5D surface:

$$f_\infty \equiv \left(\frac{H'_x}{aV'^c (1-V')^d} \right)^2 + \left(\frac{M'_y}{bV'^e (1-V')^f} \right)^2 + \left(\frac{H'_y}{aV'^c (1-V')^d} \right)^2 + \left(\frac{M'_x}{bV'^e (1-V')^f} \right)^2 - 1 = 0 \quad (3)$$

With the coefficients:

- a, b defining the size of the surface in the planes (H'-M')
- c, d, e and f defining the parabolic shape of the surface in the planes (V'-M') and (V'-H')

Theses parameters can be fitted to different experimental results found in the literature (see for example the numerical simulations presented hereafter).

The denominators for the horizontal forces (the moments) are the same. Therefore the interactions between the two horizontal forces (moments) are described by circles.

Loading surface

The loading surface used was initially developed in the work of (Crémer, 2001) to describe the behavior of a 2D shallow foundation. The adaptation for the 3D macro element is again simple, because of the circular shape of the footing. It consists in adding 2 terms in relation with the horizontal force H'_x and the moment M'_y. One finally obtains the following 5D surface:

$$f_c(F,\vec{\tau},\rho,\gamma) \equiv \left(\frac{H'_x}{\rho a V'^c (\gamma - V')^d} - \frac{\alpha}{\rho}\right)^2 + \left(\frac{M'_y}{\rho b V'^e (\gamma - V')^f} - \frac{\beta}{\rho}\right)^2 + \left(\frac{H'_y}{\rho a V'^c (\gamma - V')^d} - \frac{\delta}{\rho}\right)^2 + \left(\frac{M'_x}{\rho b V'^e (\gamma - V')^f} - \frac{\eta}{\rho}\right)^2 - 1 = 0 \quad (4)$$

Where $\vec{\tau} = (\alpha, \beta, \delta, \eta)$ is the kinematic hardening vector composed of the 4 kinematics hardening variables and ρ the isotropic hardening variable. The variable γ is chosen to parameterize the second intersection point of the loading surface with the V' axis (the other point is the origin of the space) and its evolution in the *V'* axis. This hardening variable gives the maximum vertical load that the structure supported throughout the whole history of the loading (most of the time it is equal to the weight of the structure).

Kinematic hardening rule

The kinematic variables $\alpha, \beta, \delta, \eta$ permit to determine the centre of the ellipse in the hyper plane (H'_x, M'_y, H'_y, M'_x). The evolution of theses variables has been obtained by studying the experimental and numerical behaviour of a foundation under a monotonic static loading. More specifically, (Gottardi et al., 1999) provide the relations for a circular footing and for different kinds of soils (obtained from experimental tests) and (Crémer, 2001) uses similar curves (obtained with FEM simulations) to fit her model. Figure 4 shows for example the relation between the moment M' and the rotation θ', coming from numerical simulations using the finite element code Dynaflow (Crémer, 2001). According to this diagram, the Exponential relation proposed is independent of V'.

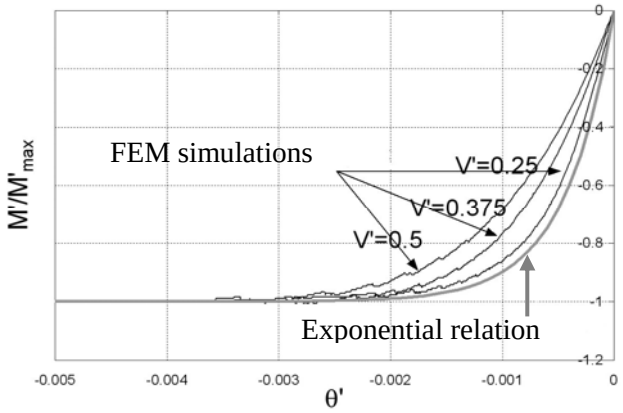

Figure 4. Relationship between moment and rocking angle using numerical simulations with the finite element code Dynaflow (Crémer, 2001)

Assuming the classical partition of the total displacement $\vec{u}$ into an elastic part $\vec{u}^{el}$ and a plastic part $\vec{u}^{pl}$ ($\vec{u} = \vec{u}^{el} + \vec{u}^{pl}$), and considering that $\dot{\vec{F}} = K^{el}\dot{\vec{u}}^{el}$, it is easy to link the increment of the forces with

the increment of the associated plastic displacements. For example, for the case of the moment one has the following equation:

$$\dot{M}'_y = K'^{el}_{\theta\theta}\left(\frac{M'^{\infty}_y}{M'_y} - 1\right)\dot{\theta}'^{pl}_y \tag{5}$$

Where M'^{∞}_y is the limit of the curve $M'_y\left(\theta'_y\right)$ when θ'_y tends to infinity.

The kinematic hardening variable β associated to this moment, is given by the following differential equation:

$$\dot{\beta} = \frac{1}{bV'^{e}\left(\gamma - V'\right)^{f}} K'^{el}_{\theta\theta}\left(\frac{M^{*\infty}_y}{\beta} - 1\right)\dot{\theta}'^{pl}_y \tag{6}$$

Where $M^{*\infty}_y$ is the limit of the curve $\beta\left(\dot{\theta}'^{pl}_y\right)$ when $\dot{\theta}'^{pl}_y$ tends to infinity. The evolutions of the other kinematic hardening variables are driven by similar relations.

As the behavior is different for $\dot{F} > 0$ and $\dot{F} < 0$, two families of kinematic hardening laws and variables are used to describe the evolution of each force. 8 relations and variables are therefore used in the model for the 8 forces $\dot{H}'_x$>0, $\dot{H}'_x$<0, $\dot{H}'_y$>0, $\dot{H}'_y$<0, $\dot{M}'_x$>0, $\dot{M}'_x$<0, $\dot{M}'_y$>0, $\dot{M}'_y$<0. For example for a radial loading, each kinematic hardening variable has the following expression (only the case of β is presented below for simplicity):

$$\begin{cases} \dot{\beta}^{\oplus} = \dfrac{1}{bV'^{e}\left(\gamma - V'\right)^{f}} K'^{el}_{\theta\theta}\left(\dfrac{M^{*\infty}_y}{\beta^{\oplus}} - 1\right)\left|\dot{\theta}'^{pl}_y\right| \\ \dot{\beta}^{\Theta} = -\dfrac{1}{bV'^{e}\left(\gamma - V'\right)^{f}} K'^{el}_{\theta\theta}\left(-\dfrac{M^{*\infty}_y}{\beta^{\Theta}} - 1\right)\left|\dot{\theta}'^{pl}_y\right| \end{cases} \tag{7}$$

The first equation of the system (Equation 7) is activated when $\dot{\beta} \geq 0$ while the second equation when $\dot{\beta} \leq 0$. The sign of $\dot{\beta}$ is identical to the sign of $\beta_{\lim} - \beta$. The tangency rule defined in (Grange et al., 2006) and (Grange et al., 2007) provides β_{lim}, whereas β is calculated during the previous step.

In order to use Equation 7 the value of $M^{*\infty}_y$ is also needed. It is evaluated as follows:

$$\begin{cases} M^{*\infty}_y = \beta_{\lim} - \beta^{\Theta} & if \quad \dot{\beta} > 0 \\ M^{*\infty}_y = -\left(\beta_{\lim} - \beta^{\oplus}\right) & if \quad \dot{\beta} < 0 \end{cases} \tag{8}$$

Note: the limit $M^{*\infty}_y$ is always positive, less or equal to 1.

Isotropic hardening rule

The independence of the directions (for $\dot{M} > 0$ and $\dot{M} < 0$) is taken into account using the specific kinematic hardening laws described in the previous paragraphs. However, one can also link the isotropic with the kinematical hardening laws (Crémer, 2001). Indeed, when a plastic state is reached during a new cycle, the plastic behavior is recovered at the same state (and with the same slope) as before (Figure 3). The evolution of the loading surfaces describing this property is given in Figure 5.

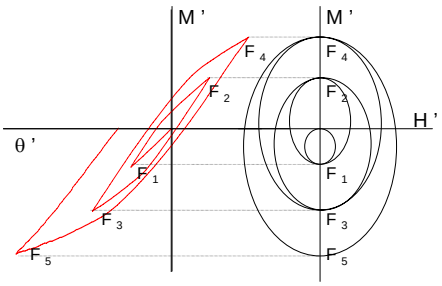

Figure 5. Evolution of the loading surfaces considering a radial loading (Crémer, 2001)

This property is translated into the following mathematical relation:

$$\dot{\rho} = \left\| \dot{\vec{\tau}} \right\| = \left| \frac{\alpha\dot{\alpha} + \beta\dot{\beta} + \delta\dot{\delta} + \eta\dot{\eta}}{\sqrt{\alpha^2 + \beta^2 + \delta^2 + \eta^2}} \right| \tag{9}$$

Evolution of γ

Its evolution is closely dependant on the evolution of the vertical force V'. During the initialization phase, where the foundation is submitted only to the weight of the structure, $\gamma = V'$. After this first phase, the evolution of γ is driven by the empirical relationship linking the vertical force and the vertical displacement given by (Nova et al., 1991). Nevertheless, the other plastic displacements (horizontal displacements and rotations) can also increase the size of the loading surfaces in the direction of V'. Consequently, the evolution of γ depends also on them according to the following expression:

$$\dot{\gamma} = K'^{el}_{zz} \left(a_1 \dot{u}'^{pl}_z + a_2 \left| \dot{u}'^{pl}_x \right| + a_3 \left| \dot{\theta}'^{pl}_y \right| + a_4 \left| \dot{u}'^{pl}_y \right| + a_5 \left| \dot{\theta}'^{pl}_x \right| \right) (1 - \gamma) \tag{10}$$

Where a_1, a_2, a_3, a_4 and a_5 are parameters which permit to adjust the influence of each component of the plastic displacement array.

Flow rule

The normality rule is defined as: $\dot{\vec{u}}^{pl} = \left\langle \dot{\lambda} \right\rangle \frac{\partial g}{\partial \vec{F}}$ where g is the flow rule and the plastic multiplier $\left\langle \dot{\lambda} \right\rangle = \dot{\lambda}$ if $\dot{\lambda} \geq 0$ and $\left\langle \dot{\lambda} \right\rangle = 0$ if $\dot{\lambda} < 0$.

A non associative flow rule is necessary (Crémer, 2001). The flow rule g used is defined by the following expression:

$$g \equiv \left(\frac{H'_x}{\rho \frac{aV'^c_0}{\left(\kappa\gamma + V'_0\right)^d} \left(\gamma - V'\right)^d \left(\kappa\gamma + V'\right)^d} - \frac{\alpha}{\rho} \right)^2 + \left(\frac{M'_y}{\rho \frac{bV'^e_0}{\left(\xi\gamma + V'_0\right)^f} \left(\gamma - V'\right)^f \left(\xi\gamma + V'\right)^f} - \frac{\beta}{\rho} \right)^2 \cdots$$

$$+ \left(\frac{H'_y}{\rho \frac{aV'^c_0}{\left(\kappa\gamma + V'_0\right)^d} \left(\gamma - V'\right)^d \left(\kappa\gamma + V'\right)^d} - \frac{\delta}{\rho} \right)^2 + \left(\frac{M'_x}{\rho \frac{bV'^e_0}{\left(\xi\gamma + V'_0\right)^f} \left(\gamma - V'\right)^f \left(\xi\gamma + V'\right)^f} - \frac{\eta}{\rho} \right)^2 \cdots \tag{11}$$

$$-1 = 0$$

The representation of g in a plane (M',V') is given by the Figure 6. A similar figure is valid in planes (H',V').

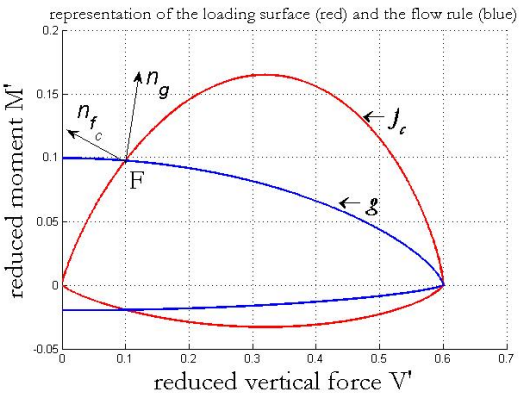

Figure 6. Representation of the computed flow rule *g*, the loading surface f_c and the corresponding normal vectors for a given loading point F in plane (M'-V')

The horizontal tangent of the flow rule can be adjusted using the 2 parameters ξ and κ in order to modify the evolutions of the plastic displacements in the hyper plane $(u'_x,\theta'_y,u'_y,\theta'_x)$.

NUMERICAL SIMULATIONS

The 3D macro element is implemented into FedeasLab, a finite element Matlab toolbox (Filippou et al., 2004). The return mapping algorithm (Simo et al., 1998) is used for the plasticity mechanism. Three different simulations are provided hereafter:

- To see whether the macro element is able to give good results under a static loading, numerical simulations are compared to experimental results coming from the works of (Gottardi et al., 1999).
- The performance of the macro element under a cyclic loading is then tested using the experimental results coming from the European program (TRISEE, 1998).
- Finally, the macro element is tested using the experimental results of the CAMUS IV structure submitted to a dynamic loading (Combescure et al., 2000), (CAFEEL-ECOEST/ICONS, 2001).

Monotonic static behavior

Detailed presentation of the tests is presented in (Gottardi et al., 1999). They concern a circular footing of diameter 2*R*=*D*=0.1m lying on a sand of a known density.

At the beginning, a vertical displacement is applied at the foundation until a given vertical force is reached. Then, the vertical displacement is kept constant while another displacement (horizontal displacement or rotation or a combined displacement) starts increasing. The test is thus completely displacement controlled. The response of the foundation is represented in the space of forces. The curve described in the space (H'_x,M'_y,H'_y,M'_x) is an approximation of the yield surface (that's the reason why the test is called "swipe test").

For the GG03 test presented hereafter, an initial vertical force V=1600N is applied followed by an increasing horizontal displacement. For the GG07 test, once a vertical force V=1600N is reached, it is reduced to V=200N. Finally, an increasing horizontal displacement is again applied.

Figure 7 and figure 8 show that the 3D macro element reproduces correctly this behavior. It is interesting to notice that the load path follows particularly well the failure criterion.

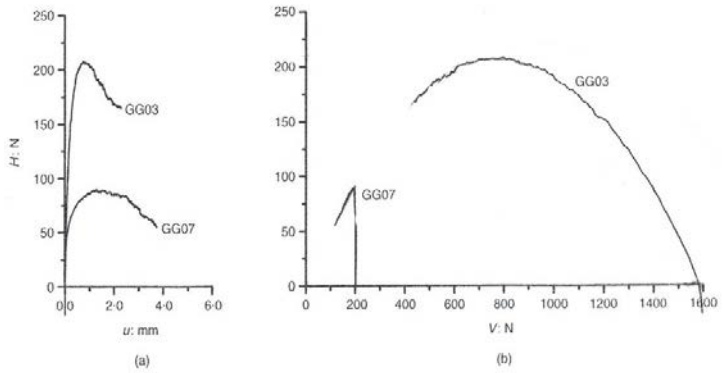

Figure 7. Experimental results for the swipe tests GG03 and GG07 in planes H_x-u_x and H_x-V

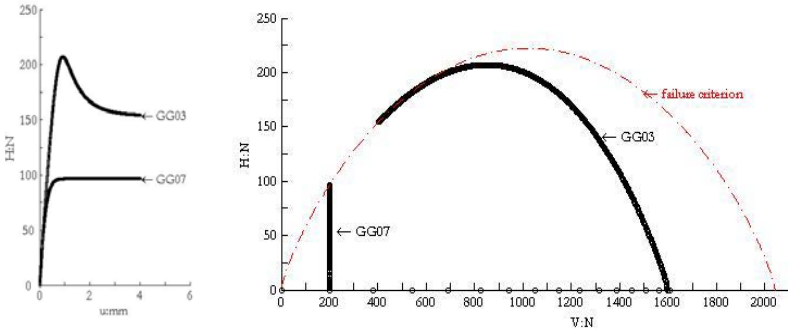

Figure 8. Numerical results for the swipe tests GG03 and GG07 in planes H_x-u_x and H_x-V

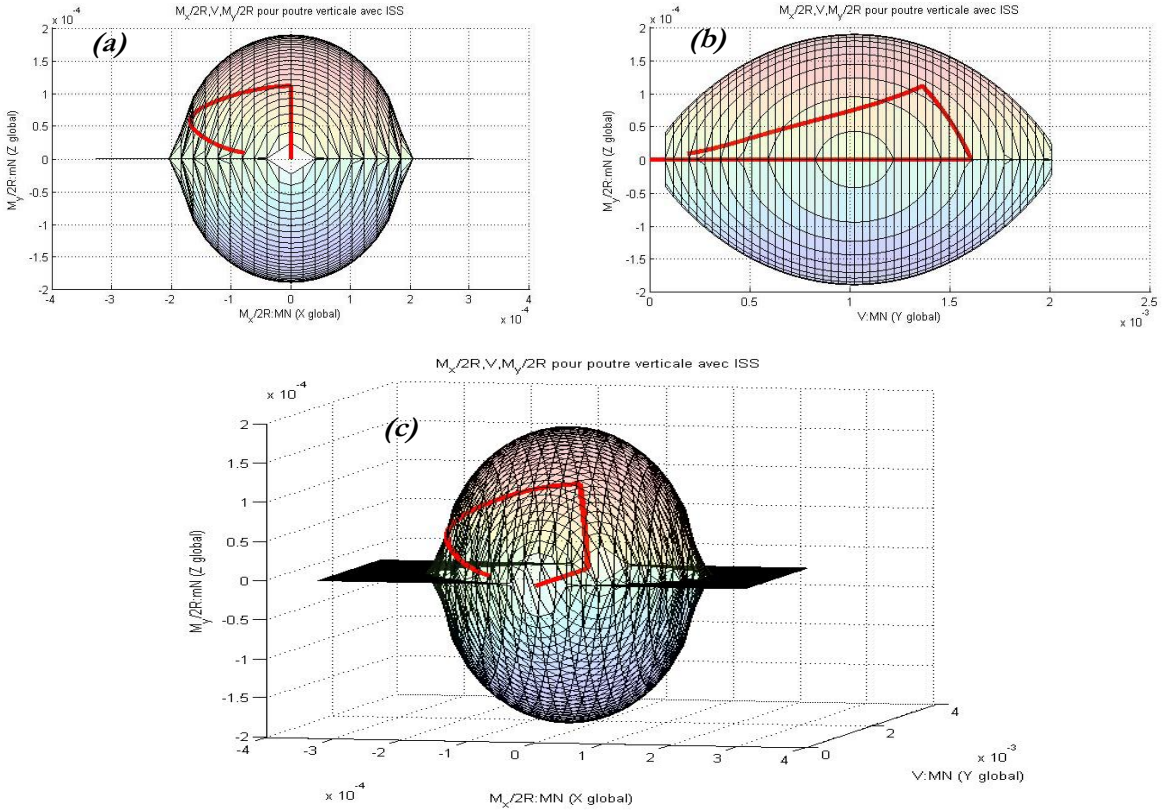

Figure 9. Numerical simulations of 3D swipe test: representation of the load path (curve in red) *(a)* in planes $M_y/2R$- $M_x/2R$, *(b)* $M_y/2R$-V, (c) in space $M_y/2R$- $M_x/2R$-V

In order to show the behavior of the macro element under a 3D loading, the following numerical 3D swipe test is performed. Figure 9 shows the load path in the ($M_x/2R$-$M_y/2R$-V) space. At the beginning, a vertical displacement is imposed till a constant value. After that, the foundation is driven with an increasing rotation θ'_y until the moment M'_y reaches a given value. Finally, θ'_y is kept constant and a new increasing rotation θ'_x is applied to the foundation. Moments in the 2 directions are clearly developed and at the end the load path is very close to the failure surface.

Cyclic static behavior

Within the European program TRISEE, experimental tests are performed on a shallow 1m x 1m rectangular foundation lying on "Low density" sand (TRISEE, 1998). Sine-shaped horizontal displacement cycles of increasing amplitude are applied at the top of a vertical beam embedded on the foundation. By imposing $\dot{\rho} = 0$ - in other words by cancelling the isotropic hardening -, it is possible to simulate this kind of behavior where no rocking is present (representative of a foundation lying on a low density soil or on a soil with low mechanical characteristics).

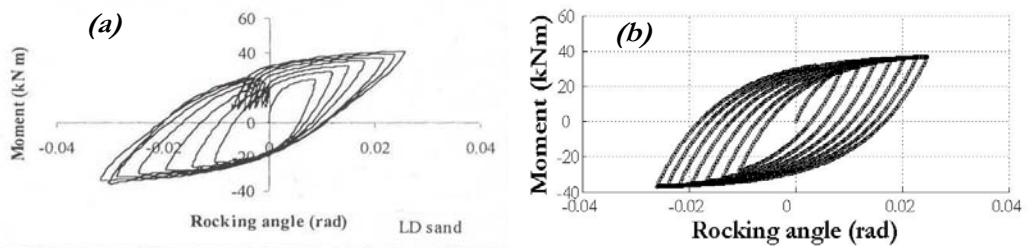

Figure 10. TRISEE: Comparison between (a) Experimental results and (b) Numerical results. Moment vs. rocking angle

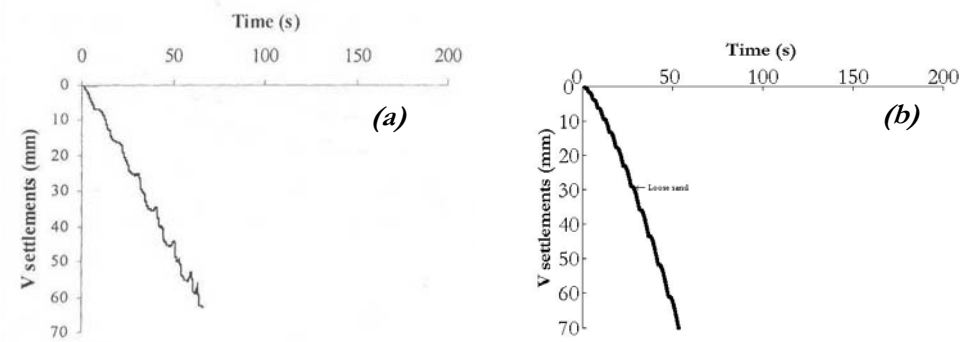

Figure 11. TRISEE: Comparison between (a) Experimental results and (b) Numerical results. Vertical settlement vs. time

Figure 10 shows the relationship between the moment and the rocking angle. Results are again very satisfactory. The main difference between the experimental and the numerical results is that for the macro element the moment reaches the asymptote (M_{lim}=40kNm) more quickly. Figure 11 presents the vertical settlement of the structure. The different plateaus of the experimental curves are well simulated by the model, thanks to the good description of the plastic displacements provided by the flow rule. Nevertheless, experimental results show that the centre of the foundation rises from time to time slightly. Of course, the macro element cannot reproduce this behavior as it can not - in its current version - simulate uplift.

Dynamic behavior

The simulation of the CAMUS IV experiment (Combescure et al., 2000) performed on the seismic table of CEA Saclay is presented hereafter in order to evaluate the efficiency of the macro element to predict the behavior of a slender structure submitted to a dynamic loading. CAMUS IV is an experiment in the line of a series carried out within the framework of the European research projects

ICONS-TMR, ECOEST II (CAFEEL-ECOEST/ICONS, 2001). The mock-up represents a 5 storey building on a 1/3 scale.

In the following graphs, the red dotted lines correspond to the experimental and the blue continuous ones to the numerical results. The structure is submitted to the earthquake motion Nice 0,33g.

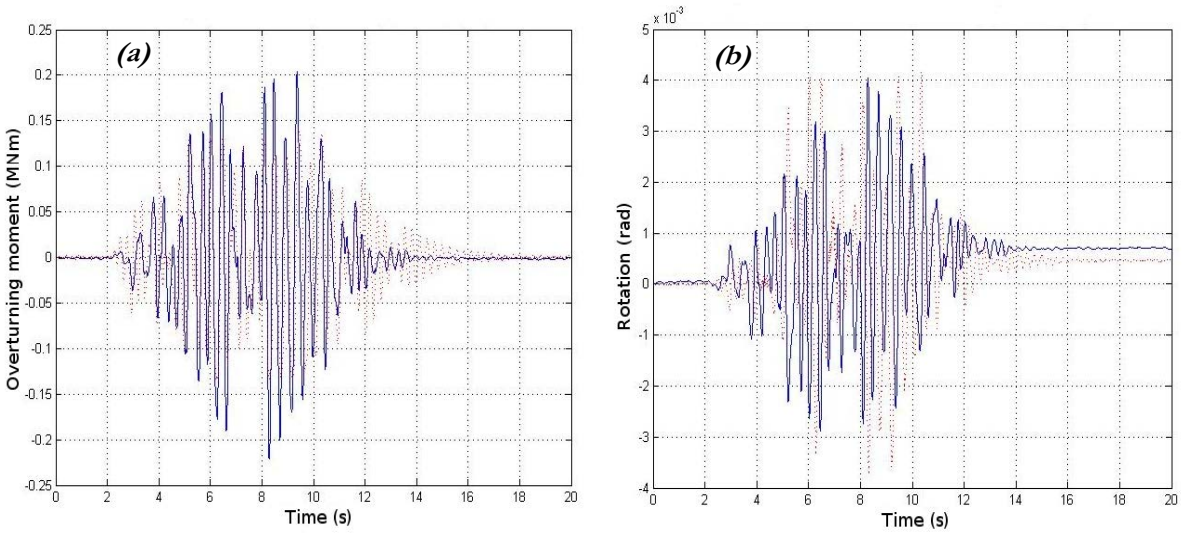

Figure 12. CAMUS IV - Evolution of (a) moment and (b) rocking angle vs. time

The main trends of the behaviour of the structure are quite well predicted (Figure 12): experimental and numerical curves are relatively in phase and the values of the moment as well as the rotation at the base are well respected. Nevertheless, some differences exist. This is possible due to the fact that uplift is not taken into account by the macro element (the specimen developed a high uplift component during the experiment). Moreover, numerical simulations considered a constant elastic stiffness. In reality, the elastic stiffness is not constant but depends on the frequency of the waves in the soil (Gazetas, 1991). It is interesting also to notice that the macro element reproduces correctly the global behaviour of the CAMUS IV specimen with a very small computational cost (only a couple of minutes are needed) and with very simple finite element mesh (21 degrees of freedom, 2D elastic beam elements are used to mesh the structure). Comparisons with the original 2D model and for the same calculations can be found in (Crémer, 2001) and (Grange, 2005).

CONCLUSION AND WAY FORWARD

The 3D macro element developed within this work gives satisfactory results for simulating the non linear behaviour of a circular swallow rigid foundation lying on an infinite space submitted to a monotonic static, cyclic or dynamic loading. Using global variables it presents the advantage of inducing low computational costs. It is implemented in the Matlab toolbox FedeasLab.
Possible improvements may deal with the fitting of the parameters (stiffness, shape of the loading surface) and the different rules (flow rule, tangency rule). The difficulty to develop a macro element in 3D lies in the fact that it has to be capable of simulating a non radial loading. In 3D indeed, forces and moments in the 2 horizontal directions *x* and *y* are coupled with a non linear relation (whereas the 2D original version of the macro element was developed by considering linearity between the horizontal force H'_x and the moment M'_y). The tangency rule, function that manages the evolution of the load surface is thus complicate and need to be improved. Uplift behavior is also an important component that has to be introduced in the formulation of the element.

AKNOWLEDGEMENTS

This research was supported within the sixth framework program (Priority 1.1.6.3 Global Change and Ecosystems) of the European Community and more specifically by the European research project LESSLOSS (Risk Mitigation for Earthquakes and Landslides Integrated Project; Project No.: GOCE-CT-2003-505488).

REFERENCES

CAFEEL-ECOEST/ICONS. Thematic report N.5. Shear Walls Structures. Editors J.M. Reynouard, M.N. Fardis, gen. eds R. T. Severn and R. Bairrão (LNEC, ISBN 972-49-1891-2) September, 2001.

Cassidy, M.J., Byrne, B.W., and Houlsby, G.T., "Modelling the behaviour of circular footings under combined loading on loose carbonate sand", Géotechnique, Vol 52, No. 10, pp. 705-712, 2002.

Combescure, D., and Chaudat, Th., ICONS european program seismic tests on r/c walls with uplift; CAMUS IV specimen - Individual Study, ICONS project Rapport, SEMT/EMSI/RT/00-27/4, CEA, Direction des Réacteurs Nucléaires, Département de Mécanique et de Technologie, 2000, Paris, France, 2000.

Crémer, C., "Modélisation du comportement non linéaire des fondations superficielles sous séismes", PhD Thesis, LMT Cachan - ENS Cachan, France, 2001.

Crémer, C., Pecker, A., and Davenne, L., "Cyclic macro element for soil-structure interaction: material and geometrical non-linearities", International Journal for Numerical and Analytical Methods in Geomechanics, Vol. 25, No. 13, pp. 1257-1284, 2001.

Crémer, C., Pecker, A., and Davenne, L., "Modelling of nonlinear dynamic behaviour of a shallow strip foundation with macro element", Journal of Earthquake Engineering, Vol. 6, No. 2, pp. 175-211, 2002.

Di Prisco, C., Galli, A., "Mechanical behaviour of shallow foundations under cyclic loads" ALERT Workshop 2006 (Without proceedings), Technical University (Politecnico) of Milan Italy, 2006.

Filippou, F.C., and Constandines, M., FedeasLab Getting Started Guide And Simulations Examples - Dpt of civil and env. Engng. UC Berkeley, 2004.

Gazetas, G., "Foundations vibrations". In Foundation Engineering Handbook, Chapter 15. Fang H-Y (ed.), van Nostrand Reinhold: New York, 1991.

Gottardi, G., Houlsby, G.T., and Butterfield, R., "Plastic response of circular footings under general planar loading", Géotechnique, Vol. 49, No. 4, pp. 453-469, 1999.

Grange, S., "Modélisation du comportement non linéaire de l'interaction sol-structure sous séisme", Master degree report, Master MCGM, UJF, INPG, 2005.

Grange, S., Kotronis, P., and Mazars, J., "Advancement of simplified modelling strategies for 3D phenomena and/or boundaries conditions for base-isolated buildings or specific soil-structure interactions". Project LESSLOSS Risk Mitigation for Earthquakes and Landslides, http://hal.ccsd.cnrs.fr/ccsd-00102513 , 2006.

Grange, S., Kotronis, P., Mazars, J., "A 3D macro-element for soil-structure interaction", International Journal for Numerical and Analytical Methods in Geomechanics, 2007 (submitted)

Nova, R., and Montrasio, L., "Settlements of shallow foundations on sand", Géotechnique, Vol. 41, No. 2, pp 243-256, 1991.

Pecker, A., Dynamique des sols. Presse, ENPC, Paris, France, 1984.

Pecker, A., "Analytical formulae for the seismic bearing capacity of shallow strip foundations", Seismic Behavior of Ground and Geotechnical Structures, Seco e Pinto (ed), pp 261-268, Balkema, Rotterdam, Netherlands, 1997.

Simo, J.C. and Hughes, T.J.R., Computational Inelasticity, Mechanics and materials, Springer Interdisciplinary applied mathematics vol.7, 1998.

TRISEE, 3D Site Effects and Soil-Foundation Interaction in Earthquake and vibration Risk Evaluation, Part 4 "Large-scale geotechnical experiments on soil-foundation interaction," European Commission, Directorate General XII for science, Research and Development, 1998.